https://doi.org/10.5194/acp-2019-617
Preprint. Discussion started: 9 August 2019


Atmospheric Chemistry and Physics Discussions

# Cloud-venting induced downward mixing of the Central African biomass burning plume during the West Africa summer monsoon

Alima Dajuma[1,3], Kehinde O. Ogunjobi[1,4], Heike Vogel[2], Peter Knippertz[2], Siélé Silué[5], Evelyne Touré N'Datchoh[3], Véronique Yoboué[3], Bernhard Vogel[2]

[1] West African Science Service Center on climate change and Adapted land Use (WASCAL)/Federal University of Technology Akure, Ondo state, Nigeria
[2] Institute of Meteorology and Climate Research, Karlsruhe Institute of Technology (KIT)
[3] University Félix Houphouët Boigny Abidjan, Côte d'Ivoire
[4] Federal University of Technology Akure (FUTA), Ondo state, Nigeria
[5]University Péléforo-Gbon-Coulibaly, Korhogo, Côte d'Ivoire

Correspondence to : Alima Dajuma (alima.dajuma@yahoo.com)

**Abstract.** Between June and September large amounts of biomass burning aerosol are released into the atmosphere from agricultural fires in Central and southern Africa. Recent studies have suggested that this plume is carried westward over the Atlantic Ocean at altitudes between 2 and 4 km and then northward with the monsoon flow at low levels to increase the atmospheric aerosol load over coastal cities in southern West Africa (SWA), thereby exacerbating air pollution problems. However, the processes by which these fire emissions are transported into the planetary boundary layer are still unclear. One potential factor is the large-scale subsidence related to the southern branch of the monsoon Hadley cell over the tropical Atlantic. Here we use convection-permitting model simulations with COSMO-ART to investigate for the first time to what extent mixing related to cloud venting contributes to the downward transport of the biomass burning plume. Based on a monthly climatology, model simulations compare satisfactory with wind fields from reanalysis data, cloud observations, and satellite retrieved CO mixing ratio. For a case study on 02 July 2016, modelled clouds and rainfall show overall good agreement with Spinning Enhanced Visible and InfraRed Imager (SEVIRI) cloud products and Global Precipitation Measurement Integrated Multi-satellite Retrievals (GPM-IMERG) rainfall estimates. However, there is a tendency for the model to produce too much clouds and rainfall over the Gulf of Guinea. Looking into the CO dispersion, used as an indicator for the biomass burning plume, we identified individual

https://doi.org/10.5194/acp-2019-617
Preprint. Discussion started: 9 August 2019


Atmospheric Chemistry and Physics Discussions

mixing events south of the coast of Côte d'Ivoire due to midlevel convective clouds injecting parts of the biomass burning plume into the boundary layer. This cloud venting is modulated by the underlying sea surface temperatures. Idealized tracer experiments suggest that about 20% of the CO mass from the 2–4km layer are mixed below 1km within two days over the Gulf of Guinea. There is even stronger vertical mixing when the biomass burning plume reaches land due to daytime heating. In that case, the long-range transported biomass burning plume is mixed with local anthropogenic emissions. Future work should provide more robust statistics on the cloud venting effect over the Gulf of Guinea and include aspects of aerosol deposition.

## 1 Introduction

The interest in air pollution over southern West Africa (SWA) has grown substantially in recent years (Knippertz et al., 2015). Population growth, urbanization, and industrialization have led to increasing local emissions from various sources in addition to natural ones. For instance, coastal city development in SWA is leading to more traffic and fuel consumption (Doumbia et al., 2018). Anthropogenic emissions will continue increasing if no regulations are implemented (Liousse et al., 2014). Domestic fires, traffic, and waste burning are the most important sources of pollution in West Africa (Marais and Wiedinmyer, 2016; Bahino et al., 2018; Djossou et al., 2018). In the framework of the Dynamics-Aerosol-Chemistry-Cloud Interactions in West Africa (DACCIWA; Knippertz et al., 2015a) field campaign in SWA during June-July 2016 (Flamant et al., 2018b), measurements of the French Service des Avions Français Instrumentés pour la Recherche en Environnement (SAFIRE) ATR-42 aircraft showed fairly high background concentrations (i.e. outside urban plumes) with PM1 mass concentrations dominated by secondary organic compounds that contribute 53% to the total aerosol mass (Brito et al., 2018). For the urban pollution plumes of Abidjan, Accra, and Lomé, they found a doubling of PM1 mass concentrations. Air pollution is a main concern for human health leading to respiratory and other diseases (Lelieveld et al., 2015) but may also affect local meteorology. For instance, Deetz et al. (2018) showed in model sensitivity experiments that increasing aerosol loadings can lead to a reduced inland penetration of the Gulf of Guinea Maritime Inflow (MI, Adler et al., 2019) and a weakening of the nocturnal low-level jet over SWA.

During the summer West African monsoon (WAM) the atmosphere over SWA is characterized by a mixture of pollutants from different sources as highlighted by Knippertz et al. (2017). In addition to the local pollution, long-range transport of dust from the Sahel and the Sahara Desert as well as biomass burning aerosol from Central and southern Africa affect the atmospheric composition. Mineral dust has been shown to affect

https://doi.org/10.5194/acp-2019-617
Preprint. Discussion started: 9 August 2019


Atmospheric Chemistry and Physics Discussions

radiation, precipitation, and many WAM features (e.g. Konare et al., 2008; Solmon et al., 2008; Stanelle et al., 2010; Raji et al., 2017; N'Datchoh et al., 2018). During this period, biomass burning is widespread in Central and southern Africa, when plumes are carried westward by a jet between 2 and 4 km (Barbosa et al., 1999; Mari et al., 2008), while in West Africa activity peaks during the dry season from October to March (N'Datchoh et al., 2015). Biomass burning is an important source of aerosols and trace gases, with an estimated emission of several thousand Tg $a^{-1}$ for tropical areas (Barbosa et al., 1999; Van der Werf et al., 2003; Ito and Penner, 2004). Hao and Liu (1994) estimated that almost half of the biomass burning from the tropics come from tropical Africa to which the savanna contributes up 30% of the global total and 64% of the African total. During the DACCIWA field campaign, a surprisingly high level of pollution was observed over the sea upstream of SWA. Haslett et al. (2019) found a significant mass of aged accumulation mode aerosol in the planetary boundary layer (PBL) over both continent and ocean. According to modelling work by Menut et al. (2018) biomass burning from Central and southern Africa increases the level of air pollution in urban cities such as Lagos and Abidjan by approximately 150 µg $m^{-3}$ for CO, 10-20 µg $m^{-3}$ for $O_3$, and 5 µg $m^{-3}$ for PM2.5.

An important and open question is the mechanism by which the biomass burning aerosols from Central Africa get from the layer of midlevel easterlies into the PBL. The hypothesis we investigate in this paper is that cloud venting plays a considerable role in the downward mixing of biomass burning aerosol. Most previous studies have focused on cloud-induced upward transport of aerosols and chemical species from close to their sources in the PBL to the free troposphere (e.g. Ching et al., 1988; Cotton et al., 1995). Using two-dimensional idealized simulations, Flossmann and Wobrock (1996) calculated the mass transport of trace gases across cloud boundaries and from the marine boundary layer into the free troposphere. They found that 60% of the mass of an inert tracer is exported due to convective clouds. The same paper also examines the transport of $SO_2$ including chemical reactions showing that only a small fraction is dissolved and reacts in the aqueous phase, while substantial amounts of $SO_2$ are redistributed by clouds (see also Kreidenweis et al., 1997). Using a 1-D entraining-detraining plume model with ice microphysics, Mari et al. (2000) studied the transport of CO (inert tracer), $CH_3COOH$, $CH_2O$, $H_2O_2$, and $HNO_3$, and compared the results with observations from the Trace and Atmospheric Chemistry Near the Equator-Atlantic (TRACE) campaign. Convective enhancement factors at 7–12 km altitude, representing the ratios of post convective to pre-convective mixing ratios, were calculated for both observed and simulated cases. Observed (simulated) values were 2.4 (1.9) for CO, 11 (9.5) for $CH_3COOH$, 2.9 (3.1) for $CH_2O$, 1.9 (1.2) for $H_2O_2$, and 0.8 (0.4) for $HNO_3$. Simulating trace gas redistribution by convective clouds, Yin et al. (2001) found abundant highly soluble gases in the uppermost parts of continental precipitating

https://doi.org/10.5194/acp-2019-617
Preprint. Discussion started: 9 August 2019


Atmospheric Chemistry and Physics Discussions

clouds. Halland et al. (2009) showed substantial vertical transport of tropospheric CO by deep mesoscale convective systems and assessed the ability of the satellite borne Tropospheric Emission Spectrometer to detect the resulting enhanced CO in the upper atmosphere.

This study will use simulations with the COSMO (consortium for small-scale modelling) model (Baldauf et al., 2011) online coupled with Aerosol and Reactive Trace gases (ART, Vogel et al., 2009) to investigate cloud-induced transports of biomass burning aerosols from mid-level tropospheric layers into the PBL over the Gulf of Guinea and SWA. A one-month simulation for July 2016 (i.e. during the DACCIWA field campaign) over a larger domain will be evaluated with available observational datasets and combined with a detailed high-resolution case study, followed by idealized tracer experiments designed to quantify the vertical transport. The paper is organized as follows. Section 2 describes the satellite and re-analysis data as well as the model framework and simulation set up used for this study. The model evaluation is presented in section 3. In section 4 the cloud venting process and its contribution to the vertical mixing of the biomass burning plume are assessed and discussed. Analysis of an artificial tracer to quantify the mass fraction of the biomass burning plume that mixes down into the PBL is given in section 5. The last section presents a summary of the results and conclusions.

## 2 Data and Modelling

### 2.1 Observational Data

The following data from space-borne platforms and reanalysis are used for this study:

1. The Moderate Resolution Imaging Spectroradiometer (MODIS) is a key instrument on board the EOS Terra satellites. The instrument views the entire Earth's surface every one to two days acquiring data in 36 spectral bands ranging in wavelengths from 0.4 µm to 14.4 µm. The MODIS product for cloud properties we use is MOD08_E3 (Platnick et al., 2017). Amongst others it contains 1x1 degree grid averaged values of cloud fraction averaged over the month of July 2016.

2. Measurement of Pollution in the Troposphere satellite (MOPITT) is used to derive CO volume mixing ratios. MOPITT measurements are performed in eight nadir-viewing spectral channels using a gas correlation spectroscopy technique with a horizontal resolution of 22x22 $km^2$ (Clerbaux et al., 2008). A detailed description

https://doi.org/10.5194/acp-2019-617
Preprint. Discussion started: 9 August 2019


Atmospheric Chemistry and Physics Discussions

of the instrument and measurement technique can be found in Drummond and Mand, 1996; Pan et al., 1998; Edwards et al., 1999). The data are available at different height levels from the surface to 150 hPa. Global coverage is reached after 3 to 4 days.

3. To represent standard meteorological fields, monthly mean ERA-Interim reanalysis data from the European Centre for Medium-Range Weather Forecasts (ECMWF) are used for this study (Dee et al., 2011).

4. Daily Sea Surface Temperatures (SST) from the National Oceanic and Atmospheric Administration (NOAA; Reynolds et al., 2007) are analyzed for the detailed case study on 02 July 2016. The SST analysis has a spatial resolution of 0.25 degrees and a temporal resolution of one day. The product uses Advanced Very High Resolution Radiometer (AVHRR) satellite data from the Pathfinder AVHRR SST dataset (Stowe et al., 2002).

5. The Global Precipitation Measurement Integrated Multi-satellite Retrievals (GPM-IMERG) product from National Aeronautics and Space Administration (NASA) is used for rainfall evaluation. It uses an algorithm that merges precipitation radar, microwave precipitation estimates, microwave-calibrated infrared, and rain gauge analyses at a spatial resolution of 0.1° over the latitudinal belt 60°N–60°S. The product has a time resolution of 30 minutes (Hou et al., 2014; Huffman et al., 2018).

All observational data (satellites and reanalysis data) are collocated with respect to time and space for the comparison with the model results.

**2.2 Modelling**

For the simulations performed in this study, the numerical weather prediction model of the Consortium for small-scale modelling (COSMO; Baldauf et al., 2011) online coupled with Aerosol and Reactive Trace gases (ART) is used (Vogel et al., 2009). COSMO-ART allows the treatment of aerosol dynamics, atmospheric chemistry, and the feedback with radiation and cloud microphysics (Vogel et al., 2009; Knote et al., 2011;Bangert et al., 2012; Athanasopoulou et al., 2013). A 1 D-plume rise model of biomass burning aerosols and gases in COSMO-ART calculates online the injection height of the biomass pollution plume and the emission strength of gases and particles (Walter et al., 2016). The parameterization scheme uses data obtained from the Global Fire Assimilation System ( GFAS v1.2; Kaiser et al., 2012), in particular MODIS satellite data of the fire radiative power. Anthropogenic emissions are taken from the Emission Database for Global Atmospheric Research Hemispheric Transport of Air Pollution version 2 (EDGAR HTAP_v2) dataset (Edgar,

https://doi.org/10.5194/acp-2019-617
Preprint. Discussion started: 9 August 2019


Atmospheric Chemistry and Physics Discussions

2011) for 2010 with a 0.1° horizontal resolution. In addition, the recently developed gas flaring emission parameterization for SWA by Deetz and Vogel (2016) was used that is based on a combination of remote sensing observations and physically based combustion equations. Biogenic emissions, sea salt, dimethyl sulfide, and mineral dust are calculated online within the model system. Meteorological initial and boundary conditions are taken from the operational global ICOsahedral Non-hydrostatic (ICON) model (Zängl et al., 2015) runs of the German Weather Service (DWD). Initial and boundary conditions for gaseous and particulate compounds are derived from Model for Ozone and Related Chemical Tracers (MOZART) forecasts (Emmons et al., 2009).

To cover a large domain including the fire areas in Central Africa on the one hand and to reach a high horizontal resolution in our area of interest (Gulf of Guinea and SWA) we used the nesting option of COSMO-ART. The modelling domains are presented in Fig. 1. The outer domain D1 (18°W–26.6°E; 20°S–24.6°N) indicated by the small box at the left bottom corner of the figure covers West Africa and the southeastern Atlantic Ocean. The red rectangle inside this box shows the location of the nested domain D2 (9°W–1°E; 3°–10.8°N), mostly covering Ivory Coast and Ghana. The color shading gives the surface height above sea level (ASL). D2 is dominated by tropical forests in the south to savanna and grassland vegetation in the north. Simulations are done on D1 with a horizontal grid spacing of 5 km and 50 verticals levels. The simulation over D2 use results of D1 as boundary and initial conditions, and are carried out with a horizontal grid spacing of 2.5 km with 80 verticals levels up to 30 km (28 levels below 1.5 km ASL).

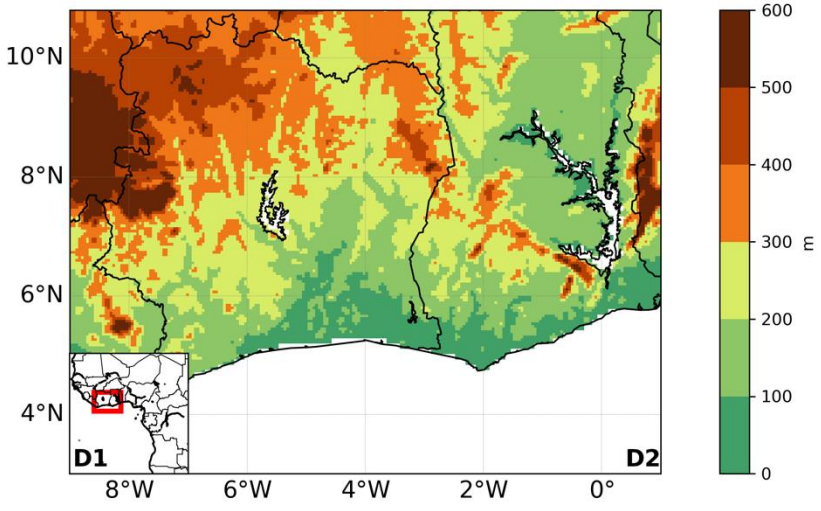

https://doi.org/10.5194/acp-2019-617
Preprint. Discussion started: 9 August 2019


Atmospheric Chemistry and Physics Discussions

*Figure 1. Geographical overview. Model domains D1 (inset) and D2 (main image). The horizontal resolution in case of D1 is 5 km and 2.5 km in case of D2. The color shading gives the surface height above sea level over D2.*

The model configuration used in this study is the same as in Deetz et al. (2018). The modelled period ranges from 25 June – 31 July 2016 over D1. We analyze a particular case study on 02–03 July simulated over D2. The purpose is to compare the model outputs and observations for monthly mean conditions over D1 and to perform detailed process studies, in particular the cloud venting over the Gulf of Guinea, for the 02-03 July 2016 case over D2. An artificial tracer experiment is performed to quantify the percentage of mass mixed from the free troposphere into the PBL. We used CO as an inert tracer and a surrogate for biomass burning emissions. The deposition velocity is set to zero and chemistry switched off in order to account only for meteorological atmospheric transport processes. The interaction between gas phase chemistry, aerosol dynamics and the meteorology is neglected. We set a constant profile of 1 ppmv at the height where the maximum concentration of the biomass burning plume is observed (i.e. 2–4 km) and 0 below and above that layer.

## 3 Model evaluation

Figure 2a shows a July 2016 average of the wind speed and streamlines at 925 hPa as simulated by COSMO-ART. Figure 2b shows the corresponding figure for the ERA-Interim re-analysis. The wind is southeasterly in the southern hemisphere and turns southwesterly along the Guinea Coast after crossing the equator. This low-level monsoon flow advects relatively cool and moist air from the Gulf of Guinea onto the continent. In July the precipitation maximum is located around 10°N (e.g. Janicot et al., 2008), and westerlies penetrate far north into the continent and over the adjacent Atlantic Ocean. Apart from a slightly northward shifted turning point, COSMO-ART agrees well with ERA-Interim in terms of the overall structure of the low-level flow field. However, there are some prominent differences in wind speed. ERA-Interim shows highest wind speeds in the southern hemisphere and a slow down towards SWA as well as a clear minimum over Central Africa. COSMO-ART shows a stronger monsoon flow and also significantly higher winds over Central Africa. Maxima reach 15 m $s^{-1}$ for both for model and reanalysis. COSMO-ART shows a domain average of 6 m $s^{-1}$, 1.4 m $s^{-1}$ higher than ERA-Interim.

https://doi.org/10.5194/acp-2019-617
Preprint. Discussion started: 9 August 2019


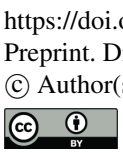

Atmospheric Chemistry and Physics Discussions

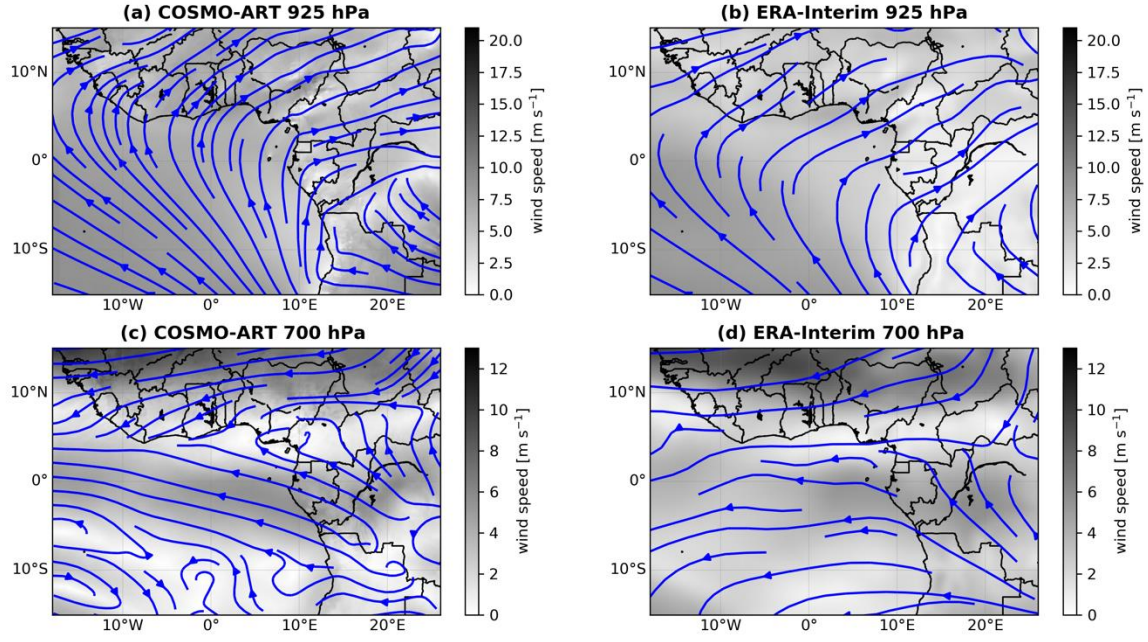


*Figure 2. Average wind speed (grey shading) and streamlines at 925hPa (top) and 700hPa (bottom) simulated with COSMO-ART (left) and in ERA-Interim re-analysis (right) for July 2016. Note the different scales in top and bottom panels.*

The wind field at 700 hPa is characterized by a broad easterly flow across most of the considered domain (Figs. 2c and d). A maximum is found over the Sahel known as the African Easterly Jet (AEJ), which typically peaks around 600 hPa (Parker et al., 2005) and is the result of the large meridional temperature gradient at low levels (Cook, 1999; Wu et al., 2009). The AEJ is well represented in COSMO-ART with a maximum wind speed of 10.9 m $s^{-1}$ as compared to 13.0 m $s^{-1}$ in ERA-Interim. Easterlies are also enhanced near the equator with weaker flow over the Guinea Coast to the north. There are some subtle differences between COSMO-ART and ERA-Interim here, with the model showing a larger northward component over the ocean and slightly stronger winds. COSMO-ART also displays more fine structure in the southern hemisphere, where winds are overall weaker. Despite the differences between COSMO-ART and ERA-Interim discussed above, we anticipate an overall realistic transport of biomass burning aerosol in the model, i.e. westward away from the hotspots in Central Africa out to the Atlantic and then northward into SWA with the monsoon flow, if downward mixing occurs.

https://doi.org/10.5194/acp-2019-617
Preprint. Discussion started: 9 August 2019


Atmospheric Chemistry and Physics Discussions

The simulated total cloud fraction averaged over July 2016 (Fig. 3a) is compared to observations from MODIS (Fig. 3b). SWA is very cloudy in summer with typical values ranging from 70% to almost 100% in agreement with multi-year values presented in Hill et al. (2016). The cloud cover is overall adequately represented by COSMO-ART over land, particularly relative to the poor performance of many coarser-resolution climate models (Hannak et al., 2017). Cloud cover maxima stretch from southwestern Ghana to northeastern Ivory Coast, along the Atakora chain at the border of Ghana and Togo, and over the Guinea Highlands of Liberia and Sierra Leone with satisfactory agreement between the two datasets. Towards the Sahel cloud fraction decreases markedly in COSMO-ART but much less so in MODIS, which has a rather prominent minimum over central Ivory Coast. Cloud cover is clearly overestimated by the model over the Gulf of Guinea with two local minima upwind of Abidjan and Accra, which may be related to coastal upwelling and are hard to verify with MODIS due to the coarser resolution. This suggests a potential overestimation of cloud venting over the ocean in the model.

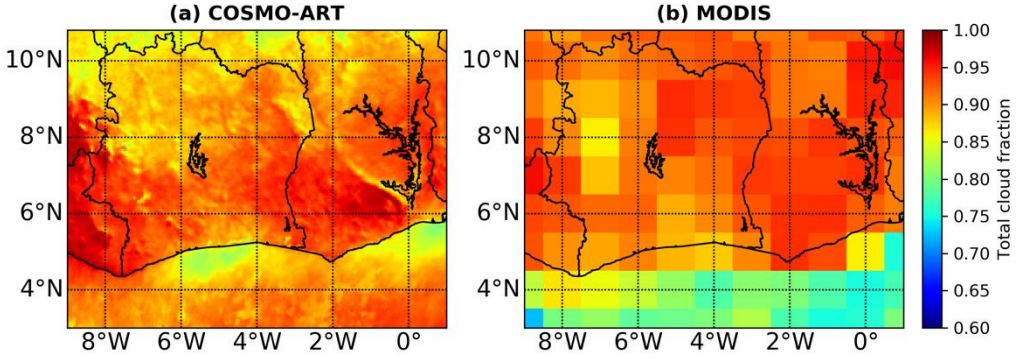


*Figure 3. Monthly mean total cloud fraction for July 2016 over domain D2 as simulated with COSMO-ART (a) and observed by MODIS (b).*

Finally, the modelled mixing ratio of surface CO is evaluated with satellite data for July 2016. Figure 4 displays the monthly mean of the modelled spatial distribution together with the CO fields observed by MOPITT. Overall the spatial patterns of CO concentration are reasonably captured by the model. Some areas have too frequent cloud contamination and do not allow the computation of a representative monthly mean (white

https://doi.org/10.5194/acp-2019-617
Preprint. Discussion started: 9 August 2019


Atmospheric Chemistry and Physics Discussions

shading in Fig. 4b). Over Central Africa widespread burning is evident with a larger magnitude and spatial extent in the model as compared to satellite. From there a plume of enhanced concentrations stretches northwestward in both datasets, but again fields in COSMO-ART are somewhat larger and therefore reach more remote parts of the Atlantic Ocean. This also supports a potential overestimation of the important of pollution from Central Africa into SWA in the model. In addition, COSMO-ART simulates marked pollution plumes over Nigeria associated with Lagos, the oil fields in the Niger Delta (flaring activities), and the population center around the Sahelian city of Kano, which are hard to verify due to clouds. Emissions from other large cities (e.g. Accra, Kumasi, Abidjan) appear relatively weak in COSMO-ART. This may be at least partly due to uncertainties in standard emission inventories (Liousse et al., 2014). Despite some overall discrepancies, we argue that the two fields are similar enough to draw conclusions on the importance of cloud-mixing process in the model, particularly because the fields are relatively similar over the ocean.

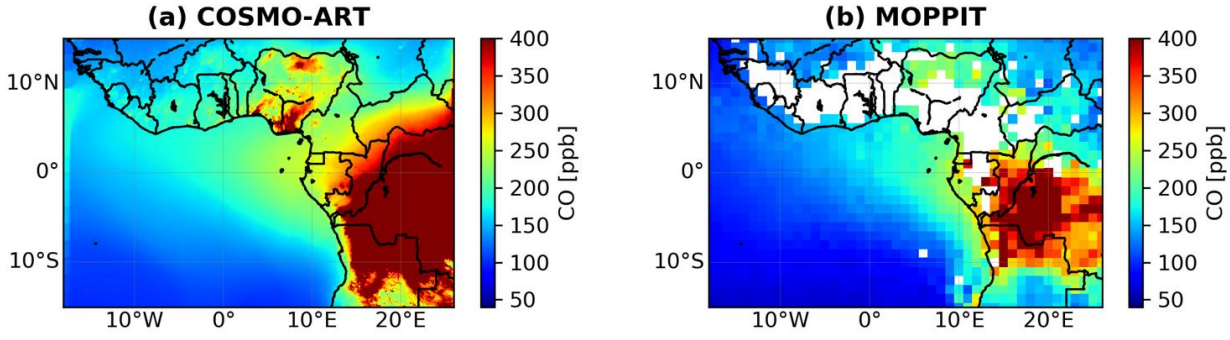


*Figure 4. Monthly mean surface CO concentrations for July 2016 as simulated by COSMO-ART (left) and as observed by MOPPIT (right).*

## 4 Case study of cloud venting

In section 3 we presented simulated monthly mean conditions. We will now focus on a case study for 02 July 2016 to illustrate the impact of meteorology on the spatial and temporal distribution of CO. We will especially focus on the role of convective clouds on the vertical distribution of CO.

https://doi.org/10.5194/acp-2019-617
Preprint. Discussion started: 9 August 2019


Atmospheric Chemistry and Physics Discussions

### 4.1 Simulated temperature distribution

The spatial distribution of simulated 2m temperature is displayed in Fig. 5 at 12 UTC on 02 July 2016. At this time of day the temperature is already higher over land than over the ocean. Local temperature maxima are located over cities such as Abidjan and Accra. High temperatures are also simulated in the central part of Ghana near Lake Volta. Modelled temperatures over the Gulf of Guinea are between 26°C and 28 °C in agreement with observed SST shown in Knippertz et al. (2017). There are clear indications of cold pools related to convective cells developing over the Gulf over Guinea. The hourly analysis of the temperature field (not shown) shows cold pools appearing around 7 UTC and persisting during the whole day. They are connected to downward motion starting at and above cloud base, bringing air and its constituents from aloft into the PBL.

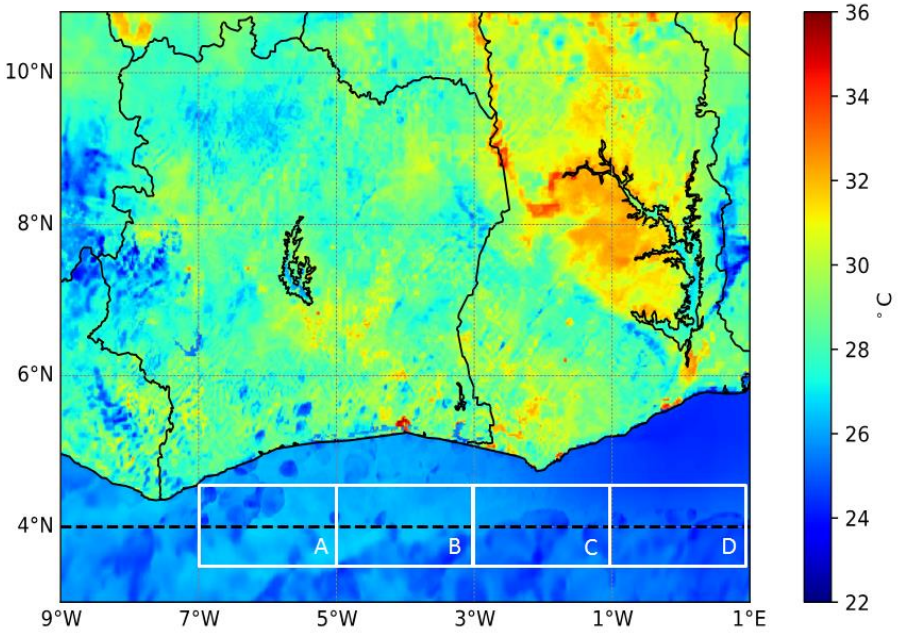


*Figure 5. 2-m temperature as simulated by COSMOS-ART over domain D2 (see Fig. 1) on 02 July 2016 at 12 UTC. Note the small-scale cold-pool signatures over the ocean. The position of the zonal cross-section in Fig. 8 is marked with a dashed line. Different subdomains are defined along 4°N (see Fig. 10): 7–5°W (A), 5–3°W (B), 3–1°W (C), and 1°W-1°E (D).*

https://doi.org/10.5194/acp-2019-617
Preprint. Discussion started: 9 August 2019


Atmospheric Chemistry and Physics Discussions

### 4.2 Spatial distribution of clouds and rainfall

Satellite retrieved images from EUMETSAT on 02 July 2016 show widespread clouds over SWA and the adjacent ocean, with convective cells located over the Gulf of Guinea south of Ivory Coast at 12 UTC (Fig. 6b). They produce rain rates of several mm $h^{-1}$ in the course of the afternoon according to GPM-IMERG (Fig. 6d). the cells over the ocean developed near the border between Ivory Coast and Ghana in the morning hours and propagated slowly westward in the course of the day (not shown). They form despite anomalously cold coastal waters but may have benefitted from substantially warmer SST along the equator (see Fig. 3 in Knippertz et al., 2017). Mostly moderate precipitation is also observed over land, in central Ghana, around Kumasi as well as along the borders between Cote d'Ivoire with Liberia, Guinea, and Mali.

Total cloud cover and precipitation as simulated by COSMO-ART for 02 July 2016 are shown in Figs. 6a and c. The whole area is dominated by clouds (Fig. 6a) with moderate gaps around Lake Volta and over the ocean upwind of Ghana and Ivory Coast. There is reasonable qualitative agreement between the model and observations (Fig. 6b) but the differences in cloud optical thickness evident from the satellite image make a detailed comparison somewhat difficult. With respect to precipitation, COSMO-ART shows substantially more fine structure than GPM-IMERG. Many localized shower are evident over Ivory Coast and neighboring countries with higher intensities over the hilly terrain in Liberia and along the land-sea breeze convergence parallel to the coast. Larger cells form in the model over the hilly terrain surrounding Lake Volta. The largest and most intense cells are simulated over the ocean with a conspicuous north–south orientation. Despite the differences in resolution there is some good qualitative agreement between model and observations in particular with respect to the maxima over central Ghana and Liberia. Convection in the north is underestimated and convection over the ocean is overestimated by COSMO-ART in agreement with the cloud biases evident from Fig. 3. The latter suggests that cloud venting may be somewhat overestimated by COSMO in this specific case, allowing only a rather qualitative assessment.

https://doi.org/10.5194/acp-2019-617
Preprint. Discussion started: 9 August 2019


Atmospheric Chemistry and Physics Discussions

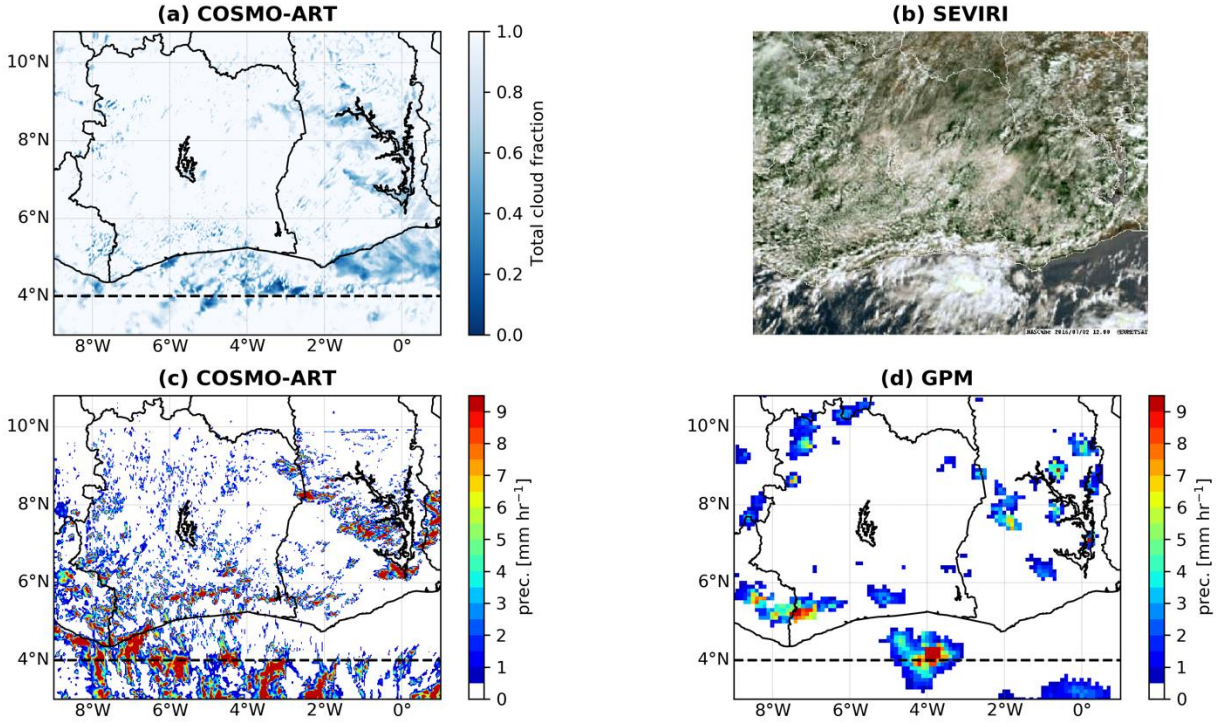


*Figure 6. Spatial distribution of clouds and rainfall over domain D2 (see Fig. 1) on 02 July 2016. (a) Total cloud fraction simulated by COSMO-ART at 12 UTC. (b) Spinning Enhanced Visible and InfraRed Imager (SEVIRI) cloud visible image from EUMETSAT at 12 UTC (from NAScube http://nascube.univ-lille1.fr). (c) Precipitation rate simulated by COSMO-ART at 18 UTC and (d) corresponding fields from the GPM–IMERG rainfall estimates. The position of the zonal cross-section in Fig. 8 is marked with dashed lines.*

### 4.3 Simulated and observed spatial distribution of CO

Figure 7 presents the simulated spatial distribution of the CO concentration for 02 July 2016, 12 UTC at 500m and roughly 3 km above the surface. At 500 m (Fig. 7a) there is a stark concentration difference between land and ocean with thick pollution plumes over the biomass burning areas in Central Africa (Barbosa et al., 1999; Mari et al, 2008; Zuidema et al., 2016) and over Nigeria. The urban plumes from coastal cities such as Abidjan, Cotonou, Lomé, and Lagos are also visible. These results come from the high anthropogenic emissions used in

https://doi.org/10.5194/acp-2019-617
Preprint. Discussion started: 9 August 2019


Atmospheric Chemistry and Physics Discussions

our study, which have maxima over Nigeria and the big cities along the coast. The simulated hourly CO concentrations (not shown here) reveal that there is a north-eastward transport of CO from the local sources in the PBL further inland with the southerly monsoon flow (Knippertz et al, 2017; Deroubaix et al., 2018). However, Flamant et al. (2018a) also showed that parts of the urban pollution re-circulate to the near coastal waters after being mixed into the midlevel easterly or sometimes northeasterly flow. Significantly lower but still considerable CO concentrations are simulated in the marine PBL over the entire eastern tropical Atlantic including the Gulf of Guinea. There is a local enhancement next to the coast stretching from Cameroon to Ivory Coast. At this height level CO is transported with the south-westerly monsoon winds from the ocean toward SWA coastal cities (see Fig. 2). Compared to the monthly mean concentration of CO (Fig. 4), 02 July was characterized by elevated pollution levels, especially over Nigeria.

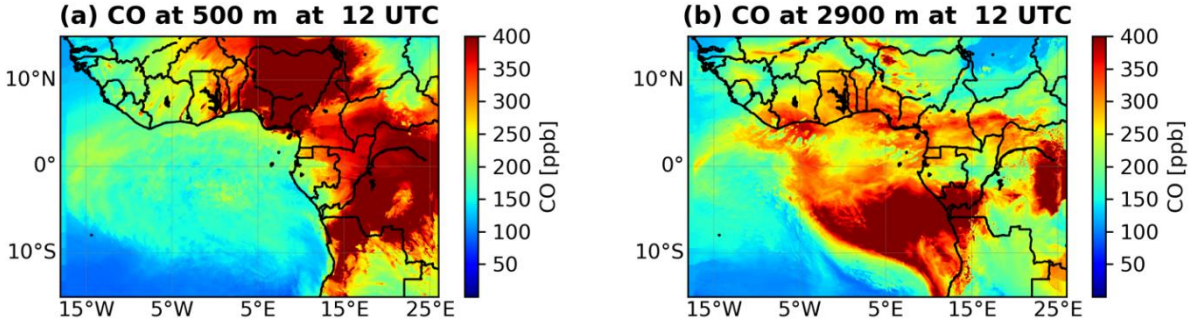


*Figure 7. CO concentrations on 02 July 2016 at 12 UTC as simulated by COSMO-ART at (a) 500m and (b) 2900 m above ground level.*

Aloft at approximately 3 km (Fig. 7b) the CO distribution is fundamentally different. Maximum CO concentrations with values of about 400 ppbv are found over the eastern Atlantic Ocean, downstream of the main burning areas in the southern hemisphere. High concentrations stretch far into SWA (e.g. into Burkina Faso), even in areas where 500m concentrations are not all that high as over Ivory Coast. This suggests a relationship to long-range transport of biomass burning plumes. This is corroborated by much reduced values in a simulation where biomass burning emissions are suppressed (not shown here). The fairly high concentrations at 500m to the west and north of the main plume at 2900m suggest downward mixing into the PBL from aloft. Subsidence within the high pressure system west of the African continent might also support the downward

https://doi.org/10.5194/acp-2019-617
Preprint. Discussion started: 9 August 2019


Atmospheric Chemistry and Physics Discussions

315 transport of CO into the boundary layer (Zuidema et al., 2016). However, the mechanism is still not clear and we will investigate in the following to what extent oceanic convective clouds support the downward mixing.

To test our hypothesis of the role of cloud venting, vertical distributions of CO concentrations and cloud liquid water content from model output are considered (Fig. 8). Figures 8a and b show simulated zonal cross sections of CO over the Gulf of Guinea at 4°N (i.e. close to the coastal cities of SWA ) over D2 on 02 July 2016 at 12
320 UTC and 18 UTC, respectively. There is a clear band of high CO concentrations of up to 400 ppbv, mostly between 1 and 3.5km over D2, which is the signature of the long-range biomass burning plumes transport from Central Africa (Mari et al, 2008; Zuidema et al, 2016), possibly affected by larger-scale subsidence.

https://doi.org/10.5194/acp-2019-617
Preprint. Discussion started: 9 August 2019


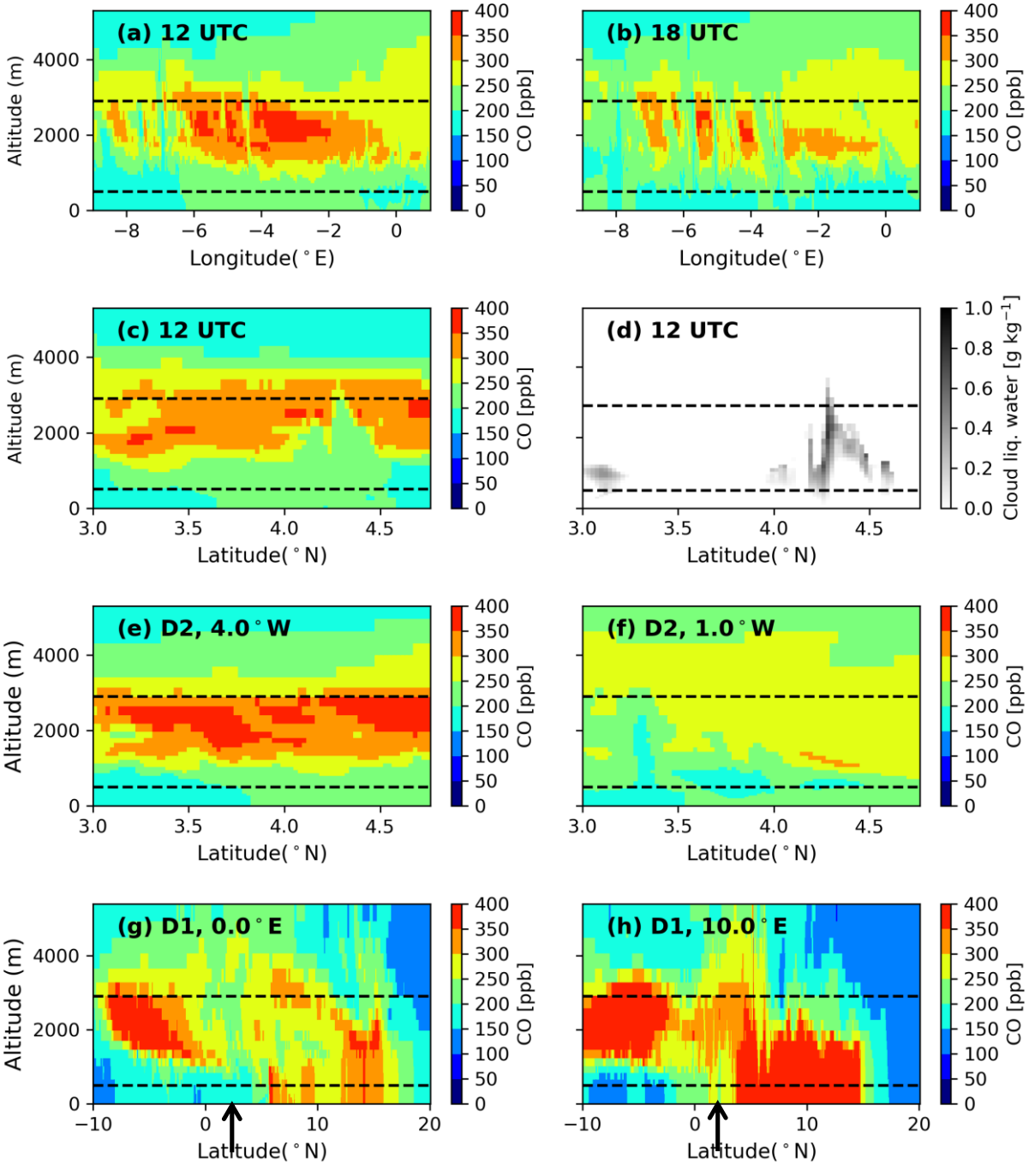

https://doi.org/10.5194/acp-2019-617
Preprint. Discussion started: 9 August 2019


Atmospheric Chemistry and Physics Discussions

*Figure 8. CO distributions as simulated by COSMO-ART over domain D1 and D2 (see Fig. 1). Zonal vertical cross-sections at 4°N of the CO concentration at (a) 12 UTC and (b) 18 UTC on 02 July 2016 for domain D2. (c) Meridional vertical cross-section at 12 UTC at 6.1°W and (d) corresponding cloud liquid water content, both for domain D2. (e) and (f) As (c) but for 4°W and 1°E, respectively. (g) and (h) Meridional vertical cross-sections over D1 at 0°E and 10°E, respectively. The height levels shown in Fig. 7 are marked by dashed lines in all panels. The arrows in (g) and (h) mark the coast line.*

The belt of high CO concentration is simulated along all longitudes of the domain but is more visible between 10°W to 0° (upwind of Cote d'Ivoire and Ghana) than between 0° E to 5°E. This corroborates the observations that the biomass burning plume is mainly advected in westerly direction (Adebiyi and Zuidema, 2016). In addition at the height of biomass burning plume, clear patterns with high horizontal concentration gradients are simulated at heights varying from around 1 km up to 4 km. These structures are more pronounced at 18 UTC (Fig. 8b). They are related to convective clouds simulated and observed (Fig. 6) over the ocean transporting CO into the PBL from above. Analyzing the simulated diurnal cycle of the vertical distribution of the CO concentration (not shown) we found that clouds appear after 7 UTC and are persistent throughout the day. Moreover, CO is also visible in the boundary layer and eventually reaches the surface. The meridional cross sections of CO (Figure 8a and b) show that concentrations below 1km can reach up to 60% of the maximum located at midlevel height due to downward mixing. Figures 8c and d show a meridional vertical cross section of the CO concentration and the specific cloud liquid water content along 6.1°W, close to where convective activity is seen in Fig. 8a. Areas of high cloud liquid water content that indicate positive and negative vertical velocities are closely related to the observed patterns in CO.

For comparison we also analyze meridional cross sections of CO corresponding to Fig. 8c but at 4°W and 1°E over domain D2. At 4°W (Fig. 8e) there is much less evidence of convective mixing than at 6.1°W and concentrations in the PBL are reduced. There is, however, a slight increase northwards that may come from turbulent mixing or advection into the section. In contrast to that, the cross-section at 1°E (Fig. 8f) shows a much weaker biomass burning plume in agreement with Fig. 7b. This appears to be the result of the bulk of the plume travelling westward over the ocean before turning northward into SWA. Also here, there are indications of a slow decent of the lower boundary of the plume that may come from subsidence or turbulent mixing. Finally it is also interesting to place the mixing near SWA into the larger regional context. Meridional cross sections along 0° and 10°E but reaching from 10°S to 20°N illustrate the full complexity of the plume evolution. At 0°E (Fig. 8g) there is a distinct biomass burning plume centered at 5°S with some indications of northward

https://doi.org/10.5194/acp-2019-617
Preprint. Discussion started: 9 August 2019


Atmospheric Chemistry and Physics Discussions

transport around 1000m AGL and individual mixing events. North of the coast (arrows in Figs. 8g and h) there is a complicated vertical structure with local near-surface emissions, overhead advection, and vertical mixing to various degrees, particular during the daytime shown here. Farther to the east at 10°E (Fig. 8h) the situation bears some similarities but the local emissions from Nigeria appear to play a larger role over land.

## 5 Artificial tracer experiments

In order to quantify the downward mixing of the biomass burning plume into the PBL by cloud venting over the Gulf of Guinea we carried out idealized numerical experiments. For the simulations initialized at 02 July 2016 at 00 UTC initial profiles of the tracer were prescribed within the domains D1 and D2. Directly at the lateral boundaries the tracer concentrations were set to zero and kept constant during the time integration. This was done to assess the horizontal transport of the tracer. The idealized tracer has a concentration of 1 ppmv between 2 and 4 km and is zero elsewhere. Chemical reactions as well as dry deposition are neglected. With this configuration the standard simulation is repeated for each case. This procedure allows to quantify the percentage of mass being mixed into the boundary layer by cloud venting that was originally located between 2 and 4 km above ground. The simulations were carried out for two days. Figure 9 shows the percentage of mass located between 2 and 4 km, below 1 km, and the sum of the two. All values are averaged between 9°W and 1°E.

Over land, i.e. between 5 and 10°N, (Fig. 9d) the vertical exchange reaches 2 km in the late morning hours. The mixing process stops when the convective boundary layer breaks down and then continues again the next morning. Tracer mass is lost due to advection out of the domain by the AEJ as shown by the declining red line. Over the ocean at 5° and 0°S (Figs. 9a and b), where mostly shallow cumuli are present, the concentration in the layer between 2 and 4 km stays almost constant. The increase of the concentration in the layer below 1 km is mostly due to horizontal transport, either from CO that is mixed into the PBL farther south or over Central Afrika itself before a westward transport. This leads to a net increase in the sum of the two layers reaching above 100% at the end of the two period considered in Fig. 9.

Over the Gulf of Guinea between 4 and 4.7°N there is a clear decrease of CO in the layer between 2 and 4 km and an increase of mass below 1 km. As the temperature of the sea surface stays constant over the course of the day and the boundary layer usually stays rather shallow, this increase is due to downward mixing due to convective clouds as illustrated above.

https://doi.org/10.5194/acp-2019-617
Preprint. Discussion started: 9 August 2019


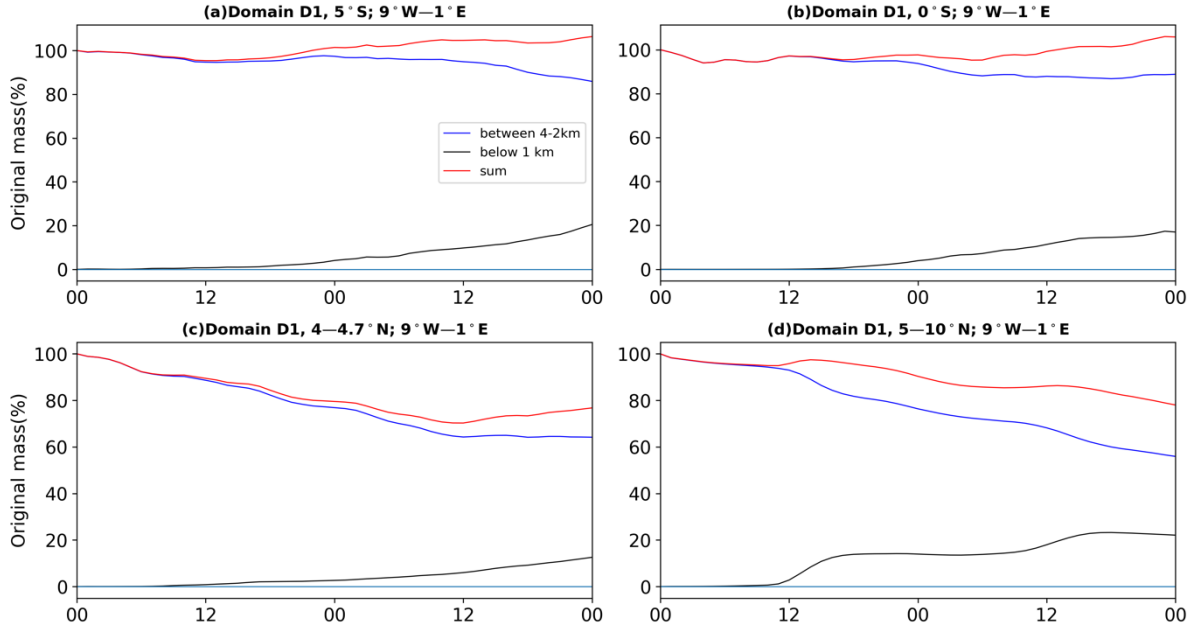


*Figure 9. Time evolution of the idealized tracer experiment on 02 and 03 July 2016 over Domain D1. Shown are changes in original mass in % between 2 and 4km (blue), below 1km (black), and the sum between the two (red). Fields are averaged from 9°W–1°E along (a) 5°S (southeastern Atlantic), (b) 0° (equatorial cold tongue), (c) 4–4.7°N (Gulf of Guinea), and (d) 5–10°N (inland SWA).*

https://doi.org/10.5194/acp-2019-617
Preprint. Discussion started: 9 August 2019


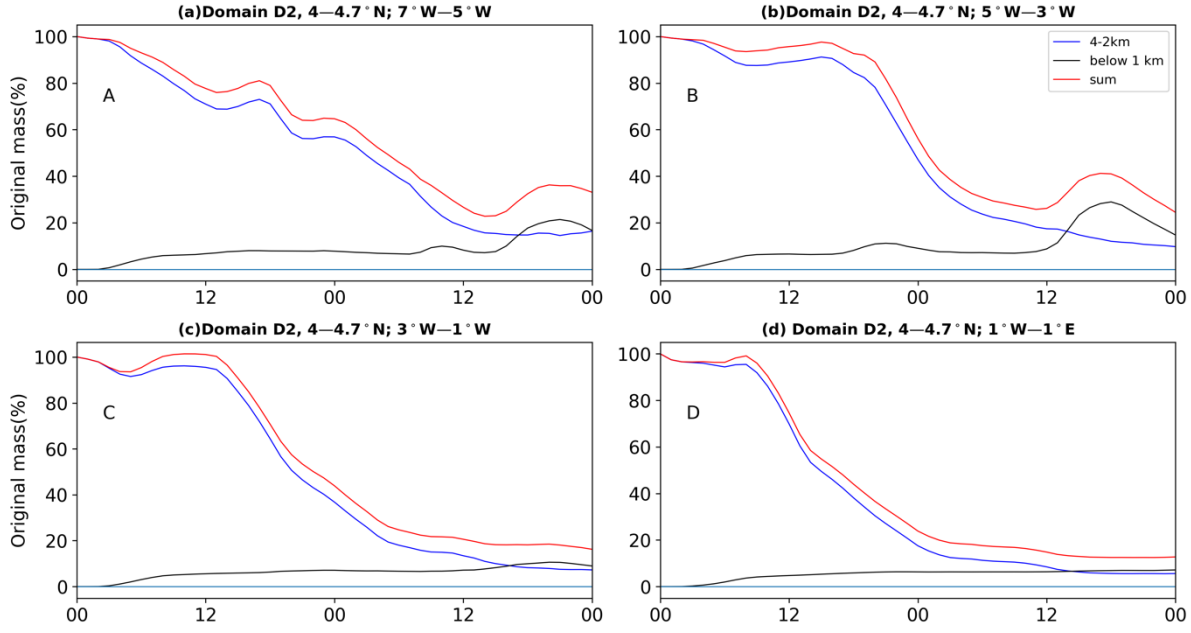


*Figure 10. Time evolution of the idealized tracer experiment on 02 and 03 July 2016 over Domain D2. Shown are changes in original mass in % between 2 and 4km (blue), below 1km (black) and the sum between the two (red). Fields are averaged from 4 –4.7°N along subdomains according to Fig. 5 (a) A, (b) B, (c) C and (d) D.*

Figure 10 shows results for the model domain D2 and for the areas A–D indicated in Fig. 5. In this configuration, the marked decrease of the tracer concentration in the layer between 2 and 4 km above surface is partly due to the vertical mixing induced by convective clouds and partly due to the advection of low concentrations from the lateral boundary. The latter is indicated by a consistently faster depletion from east to west, i.e. from D to A. The former is evident from marked individual mixing events, leading to bumps in the below 1km layer. This is a strong indication that cloud venting does in fact contribute to mixing biomass burning aerosol into the PBL.

To investigate this further, Fig. 11 shows the final mixing state in the layer below 1km after two days of integration, i.e. the right-hand-side intercept of the black curves in Fig. 9 but for steps of 1° latitude. Plotted against SSTs for the same longitudinal range, a clear correspondence is evident. Both mixing and SSTs have a

https://doi.org/10.5194/acp-2019-617
Preprint. Discussion started: 9 August 2019


Atmospheric Chemistry and Physics Discussions

marked minimum around 2°S. To the south of this SSTs increase moderately but the CO mass fraction is largely enhanced (>27%), while to the north SSTs are strongly increased but not so much the mass mixing (14–17%). This is likely a reflection of the much larger CO concentrations aloft in the southern area (see Fig. 7). The possibly more effective cloud venting in the north is not able to compensate this effect.

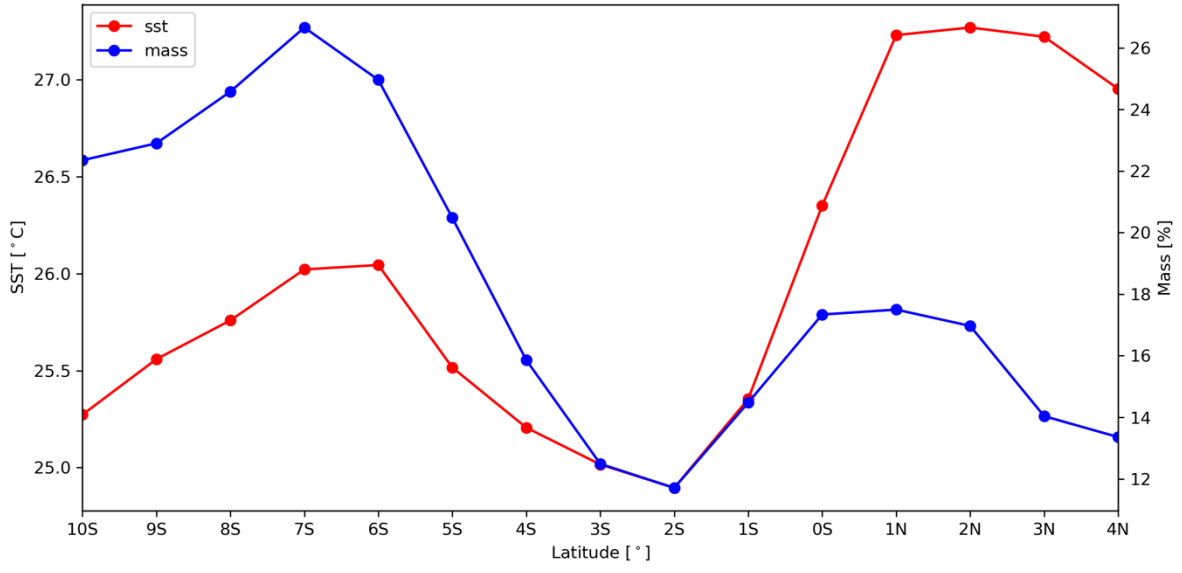


*Figure 11. Relationship between sea surface temperatures (SST) and vertical mixing of CO. CO masses in % (in blue) correspond to the values for the below 1-km layer at the end of the time window shown in Fig. 9 but for steps of one degree latitude. SSTs (in red) are from the Advanced Very High-Resolution Radiometer (AVHRR) and were averaged in the same way as the CO fields.*

## 6 Summary and conclusions

Recent observational and modelling work has revealed significant concentrations of biomass burning aerosol reaching SWA in the PBL (Brito et al., 2018; Menut et al. 2018; Haslett et al., 2019). It has been suggested that this plume stems from the extensive fires in Central Africa during the WAM season. Here we investigated

https://doi.org/10.5194/acp-2019-617
Preprint. Discussion started: 9 August 2019


Atmospheric Chemistry and Physics Discussions

potential transport pathways of the aerosol with a particular focus on the role of clouds in vertical mixing over the Gulf of Guinea. This study heavily relied on high-resolution simulations using the COSMO-ART model. While previous studies discussed subsidence to the west of the African continent to be an important mechanism, here and to the best of our knowledge we identify for the first time that cloud venting is one of the processes by which the biomass burning plume from midlevel tropospheric layers is mixed into the PBL over the Gulf of Guinea.

COSMO-ART enables us to simulate the meteorological fields over SWA and CO distribution. The simulated wind speed and direction are broadly in agreement with the ERA-Interim reanalysis, although COSMO revealed a somewhat stronger midlevel export from Central Africa and faster monsoon flow. Regarding cloud cover, COSMO-ART reproduces areas of maximum and minimum clouds over SWA but overestimates it over the Gulf of Guinea. The spatial distribution of CO is analyzed used as a tracer to detect biomass burning plumes at different heights. Compared to observations, the simulated CO concentration represents quite well areas of high values such as Central Africa where biomass burning takes place. However, the model overestimates CO concentration over Nigeria as a result of anthropogenic emissions used by the model. In the PBL, high CO concentration, have been identified over the Gulf of Guinea close to the coastal cities of SWA.

For a particular case study (02 July 2016), cold pools are found in the model over the Gulf of Guinea as a consequence of convective cells. These are also observed in satellite rainfall estimates but not quite as intense as in the model. Cross sections of CO concentration and cloud liquid water over the Gulf of Guinea give clear evidence that precipitating clouds are responsible of injecting the biomass burning plume from the mid-troposphere into the PBL. The meridional cross section of CO reveals that right below 1km, concentration can reach up to 60% of the maximum located at midlevel height due to downward mixing. The vertical transport moves biomass burning aerosol and trace gases from the westward moving main pollution layer at 2–4km, into the monsoon layer from where southerly flow can carry it into SWA and increase local pollution levels there (Haslett et al, 2019). In addition, an idealized tracer experiment shows that the leakage of biomass burning CO from the 2–4 km layer to below 1 km is on the order of 20% but varies depending on the SST.

This study is largely based on a case study to investigate the cloud venting happening over the Gulf of Guinea. More investigations of cloud venting are needed through longer simulations to get more robust statistics and through comparison with other models. Moreover, the tracer experiment has been performed for an inert tracer such as CO with no sedimentation and no deposition. Biomass burning plumes contains a lot of aerosols, which

https://doi.org/10.5194/acp-2019-617
Preprint. Discussion started: 9 August 2019




do sediment and can be washed out by rainfall into the ocean. The magnitude of this, however, remains an open question that needs to be addressed.

**Authors Contributions.** D.A., B.V., K.O. and V.Y. conceived and designed the study. D.A., B.V. and H.V. developed the model codes and carried out the simulations. D.A., P.K., B.V., and K.O. contributed to the literature, data analysis/interpretation and manuscript writing. P.K., B.V., S.S., E.T.N., and V.Y. contributed to the manuscript revision.

**Competing interests**. The authors declare that they have no conflict of interest.

**Acknowledgments**. The research leading to these results has received funding from West African Climate Science Service for Climate Change and Adapted Land Use (WASCAL) and got support from European Union 7th Framework Programme (FP7/2007-2013) under Grant Agreement no. 603502 (EU project DACCIWA: Dynamics-aerosol-chemistry-cloud interactions in West Africa). The author would like to thank Aerosols, Trace Gases and Climate Processes, Institute of Meteorology and Climate Research –Department Troposphere Research (IMK-TRO) research group for hosting her during one year at Karsruhe institute of Technology (KIT) and for their valuable contribution to the paper.

## References

Adebiyi, A. A. and Zuidema, P.: The role of the southern African easterly jet in modifying the southeast Atlantic aerosol and cloud environments, Q. J. R. Meteorol. Soc., doi:10.1002/qj.2765, 2016.

Adler, B., Babia, K., Kalthoff, N., Lohou, F., Lothon, M., Dione, C., Pedruzo-Bagazgoitia, X. and Andersen, H.:



Nocturnal low-level clouds in the atmospheric boundary layer over southern West Africa: An observation-based analysis of conditions and processes, Atmos. Chem. Phys., 19(1), 663–681, doi:10.5194/acp-19-663-2019, 2019.

Athanasopoulou, E., Vogel, H., Vogel, B., Tsimpidi, A. P., Pandis, S. N., Knote, C. and Fountoukis, C.: Modeling the meteorological and chemical effects of secondary organic aerosols during an EUCAARI campaign, Atmos. Chem. Phys., 13(2), 625–645, doi:10.5194/acp-13-625-2013, 2013.

Bahino, J., Yoboué, V., Galy-Lacaux, C., Adon, M., Akpo, A., Keita, S., Liousse, C., Gardrat, E., Chiron, C., Ossohou, M., Gnamien, S. and Djossou, J.: A pilot study of gaseous pollutants' measurement (NO2, SO2, NH3, HNO3 and O3) in Abidjan, Côte d'Ivoire: Contribution to an overview of gaseous pollution in African cities, Atmos. Chem. Phys., 18(7), 5173–5198, doi:10.5194/acp-18-5173-2018, 2018.

Baldauf, M., Seifert, A., Förstner, J., Majewski, D., Raschendorfer, M. and Reinhardt, T.: Operational Convective-Scale Numerical Weather Prediction with the COSMO Model: Description and Sensitivities, Mon. Weather Rev., doi:10.1175/MWR-D-10-05013.1, 2011.

Bangert, M., Nenes, A., Vogel, B., Vogel, H., Barahona, D., Karydis, V. A., Kumar, P., Kottmeier, C. and Blahak, U.: Saharan dust event impacts on cloud formation and radiation over Western Europe, Atmos. Chem. Phys., 12(9), 4045–4063, doi:10.5194/acp-12-4045-2012, 2012.

Brito, J., Freney, E., Dominutti, P., Borbon, A., Haslett, S. L., Batenburg, A. M., Colomb, A., Dupuy, R., Denjean, C., Burnet, F., Bourriane, T., Deroubaix, A., Sellegri, K., Borrmann, S., Coe, H., Flamant, C., Knippertz, P. and Schwarzenboeck, A.: Assessing the role of anthropogenic and biogenic sources on PM 1 over southern West Africa using aircraft measurements, Atmos. Chem. Phys, doi:10.5194/acp-18-757-2018, 2018.

Ching, J. K. S., Shipley, S. T. and Browell, E. V.: Evidence for cloud venting of mixed layer ozone and aerosols, Atmos. Environ., doi:10.1016/0004-6981(88)90030-3, 1988.

Clerbaux, C., George, M., Turquety, S., Walker, K. A., Barret, B., Bernath, P., Boone, C., Borsdorff, T., Cammas, J. P., Catoire, V., Coffey, M., Coheur, P. F., Deeter, M., De Mazière, M., Drummond, J., Duchatelet, P., Dupuy, E., De Zafra, R., Eddounia, F., Edwards, D. P., Emmons, L., Funke, B., Gille, J., Griffith, D. W. T., Hannigan, J., Hase, F., Höpfner, M., Jones, N., Kagawa, A., Kasai, Y., Kramer, I., Le Flochmoën, E., Livesey, N. J., López-Puertas, M., Luo, M., Mahieu, E., Murtagh, D., Nédélec, P., Pazmino, A., Pumphrey, H., Ricaud,

https://doi.org/10.5194/acp-2019-617
Preprint. Discussion started: 9 August 2019




P., Rinsland, C. P., Robert, C., Schneider, M., Senten, C., Stiller, G., Strandberg, A., Strong, K., Sussmann, R., Thouret, V., Urban, J. and Wiacek, A.: CO measurements from the ACE-FTS satellite instrument: Data analysis and validation using ground-based, airborne and spaceborne observations, Atmos. Chem. Phys., 8(9), 2569–2594, doi:10.5194/acp-8-2569-2008, 2008.

Cook, K. H.: Generation of the African easterly jet and its role in determining West African precipitation, J. Clim., doi:10.1175/1520-0442(1999)012<1165:GOTAEJ>2.0.CO;2, 1999.

Cotton, W. R., Alexander, G. D., Hertenstein, R., Walko, R. L., McAnelly, R. L. and Nicholls, M.: Cloud venting - A review and some new global annual estimates, Earth Sci. Rev., 39(3–4), 169–206, doi:10.1016/0012-8252(95)00007-0, 1995.

Dee, D. P., Uppala, S. M., Simmons, A. J., Berrisford, P., Poli, P., Kobayashi, S., Andrae, U., Balmaseda, M. A., Balsamo, G., Bauer, P., Bechtold, P., Beljaars, A. C. M., van de Berg, L., Bidlot, J., Bormann, N., Delsol, C., Dragani, R., Fuentes, M., Geer, A. J., Haimberger, L., Healy, S. B., Hersbach, H., Hólm, E. V., Isaksen, L., Kållberg, P., Köhler, M., Matricardi, M., Mcnally, A. P., Monge-Sanz, B. M., Morcrette, J. J., Park, B. K., Peubey, C., de Rosnay, P., Tavolato, C., Thépaut, J. N. and Vitart, F.: The ERA-Interim reanalysis: Configuration and performance of the data assimilation system, Q. J. R. Meteorol. Soc., 137(656), 553–597, doi:10.1002/qj.828, 2011.

Deetz, K. and Vogel, B.: Development of a new gas flaring emission data set for southern West Africa, Geosci. Model Dev. Discuss., doi:10.5194/gmd-2016-110, 2016.

Deetz, K., Vogel, H., Knippertz, P., Adler, B., Taylor, J., Coe, H., Bower, K., Haslett, S., Flynn, M., Dorsey, J., Crawford, I., Kottmeier, C. and Vogel, B.: Cloud and aerosol radiative effects as key players for anthropogenic changes in atmospheric dynamics over southernWest Africa, Atmos. Chem. Phys. Discuss., doi:10.5194/acp-2018-186, 2018.

Deroubaix, A., Menut, L., Flamant, C., Brito, J., Denjean, C., Dreiling, V., Fink, A., Jambert, C., Kalthoff, N., Knippertz, P., Ladkin, R., Mailler, S., Maranan, M., Pacifico, F., Piguet, B., Siour, G. and Turquety, S.: Diurnal cycle of coastal anthropogenic pollutant transport over southern West Africa during the DACCIWA campaign, , (August), 1–44, 2018.

Djossou, J., Léon, J. F., Barthélemy Akpo, A., Liousse, C., Yoboué, V., Bedou, M., Bodjrenou, M., Chiron, C.,

https://doi.org/10.5194/acp-2019-617
Preprint. Discussion started: 9 August 2019




Galy-Lacaux, C., Gardrat, E., Abbey, M., Keita, S., Bahino, J., N'Datchoh, E. T., Ossohou, M. and Awanou, C. N.: Mass concentration, optical depth and carbon composition of particulate matter in the major southern West African cities of Cotonou (Benin) and Abidjan (Côte d'Ivoire), Atmos. Chem. Phys., 18(9), 6275–6291, doi:10.5194/acp-18-6275-2018, 2018.

Doumbia, M., Toure, N. E., Silue, S., Yoboue, V., Diedhiou, A. and Hauhouot, C.: Emissions from the road traffic of West African cities: Assessment of vehicle fleet and fuel consumption, Energies, 11(9), 1–16, doi:10.3390/en11092300, 2018.

Drummond, J. R. and Mand, G. S.: The measurements of pollution in the troposphere (MOPITT) instrument: Overall performance and calibration requirements, J. Atmos. Ocean. Technol., 13(2), 314–320, doi:10.1175/1520-0426(1996)013<0314:TMOPIT>2.0.CO;2, 1996.

Edgar: EDGAR - Emission Database for Global Atmospheric Research, Glob. Emiss. EDGAR v4.2 (November 2011), doi:10.2904/EDGARv4.2, 2011.

Edwards, D. P., Halvorson, C. M. and Gille, J. C.: Radiative transfer modeling for the EOS Terra satellite Measurement of Pollution in the Troposphere (MOPITT) instrument, J. Geophys. Res. Atmos., 104(D14), 16755–16775, doi:10.1029/1999JD900167, 1999.

Emmons, L. K., Walters, S., Hess, P. G., Lamarque, J.-F., Pfister, G. G., Fillmore, D., Granier, C., Guenther, A., Kinnison, D., Laepple, T., Orlando, J., Tie, X., Tyndall, G., Wiedinmyer, C., Baughcum, S. L. and Kloster, S.: MOZART-4 description Geoscientific Model Development Discussions Description and evaluation of the Model for Ozone and Related chemical Tracers, version 4 (MOZART-4) MOZART-4 description MOZART-4 description, Geosci. Model Dev. Discuss, 2009.

Flamant, C., Deroubaix, A., Chazette, P., Brito, J., Gaetani, M., Knippertz, P., Fink, A. H., de Coetlogon, G., Menut, L., Colomb, A., Denjean, C., Meynadier, R., Rosenberg, P., Dupuy, R., Dominutti, P., Duplissy, J., Bourrianne, T., Schwarzenboeck, A., Ramonet, M. and Totems, J.: Aerosol distribution in the northern Gulf of Guinea: local anthropogenic sources, long-range transport, and the role of coastal shallow circulations, Atmos. Chem. Phys., 18(16), 12363–12389, doi:10.5194/acp-18-12363-2018, 2018a.

Flamant, C., KniPPertz, P., Fink, A. H., Akpo, A., BrooKs, B., CHiu, C. J., Coe, H., Danuor, S., Evans, M., JegeDe, O., Kalthoff, N., Konaré, A., Liousse, C., Lohou, F., Mari, C., Schlager, H., Schwarzenboeck, A.,

https://doi.org/10.5194/acp-2019-617
Preprint. Discussion started: 9 August 2019




Adler, B., Amekudzi, L., Aryee, J., Ayoola, M., BatenBurg, A. M., BessarDon, G., Borrmann, S., Brito, J., Bower, K., Burnet, F., Catoire, V., ColomB, A., DenJean, C., Fosuamankwah, K., Hill, P. G., Lee, J., Lothon, M., Maranan, M., Marsham, J., Meynadier, R., Ngamini, J. B., Rosenberg, P., Sauer, D., Smith, V., Stratmann, G., Taylor, J. W., Voigt, C. and Yoboué, V.: The dynamics⇓aerosol⇓chemistry⇓cloud interactions in west Africa field campaign, Bull. Am. Meteorol. Soc., 99(1), doi:10.1175/BAMS-D-16-0, 2018b.

Flossmann, A. I. and Wobrock, W.: Venting of gases by convective clouds, J. Geophys. Res., 101(D13), 18639, doi:10.1029/96JD01581, 1996.

Halland, J. J., Fuelberg, H. E., Pickering, K. E. and Luo, M.: Identifying convective transport of carbon monoxide by comparing remotely sensed observations from TES with cloud modeling simulations, Atmos. Chem. Phys., 9(13), 4279–4294, doi:10.5194/acp-9-4279-2009, 2009.

Hannak, L., Knippertz, P., Fink, A. H., A., K. and G., P.: AMERICAN METEOROLOGICAL This is a preliminary PDF of the author-produced, Am. Meteorogical Soc., doi:10.1175/JCLI-D-16-0451.1, 2017.

HAO, W. M. and LIU, M. H.: SPATIAL AND TEMPORAL DISTRIBUTION OF TROPICAL BIOMASS BURNING, Global Biogeochem. Cycles, doi:10.1029/94GB02086, 1994.

Haslett, S. L., Taylor, J. W., Evans, M., Morris, E., Vogel, B., Dajuma, A., Brito, J., Batenburg, A. M., Borrmann, S., Schneider, J., Schulz, C., Denjean, C., Bourrianne, T., Knippertz, P., Dupuy, R., Schwarzenböck, A., Sauer, D., Flamant, C., Dorsey, J., Crawford, I. and Coe, H.: Remote biomass burning dominates southern West African air pollution during the monsoon, Atmos. Chem. Phys. Discuss., 3(April), 1–23, doi:10.5194/acp-2019-38, 2019.

Hill, P. G., Allan, R. P., Chiu, J. C. and Stein, T. H. M.: Journal of Geophysical Research : Atmospheres and comparison to climate models, J. Geophys. Res. Atmos., 1–23, doi:10.1002/2016JD025246.Received, 2016.

Hou, A. Y., Kakar, R. K., Neeck, S., Azarbarzin, A. A., Kummerow, C. D., Kojima, M., Oki, R., Nakamura, K. and Iguchi, T.: The global precipitation measurement mission, Bull. Am. Meteorol. Soc., 95(5), 701–722, doi:10.1175/BAMS-D-13-00164.1, 2014.

Huffman, G. J., Bolvin, D. T., Braithwaite, D., Hsu, K., Joyce, R., Kidd, C., Nelkin, E. J., Sorooshian, S., Tan, T. and Xie, P.: NASA Global Precipitation Measurement (GPM) Integrated Multi-satellitE Retrievals for GPM

https://doi.org/10.5194/acp-2019-617
Preprint. Discussion started: 9 August 2019




(IMERG), Algorithm Theor. Basis Doc., (February), 1–31, doi:https://pmm.nasa.gov/resources/documents/gpm-integrated-multi-satellite-retrievals-gpm-imerg-algorithm-theoretical-basis-, 2018.

Ito, A. and Penner, J. E.: Global estimates of biomass burning emissions based on satellite imagery for the year 2000, J. Geophys. Res. D Atmos., 109(14), 1–18, doi:10.1029/2003JD004423, 2004.

Janicot, S., Thorncroft, C. D., Ali, A., Asencio, N., Berry, G., Bock, O., Bourles, B., Caniaux, G. and Chauvin, F.: ReviewAMMA field experiment in 2006.pdf, , 2569–2595, 2008.

Kaiser, J. W., Heil, A., Andreae, M. O., Benedetti, A., Chubarova, N., Jones, L., Morcrette, J. J., Razinger, M., Schultz, M. G., Suttie, M. and Van Der Werf, G. R.: Biomass burning emissions estimated with a global fire assimilation system based on observed fire radiative power, Biogeosciences, doi:10.5194/bg-9-527-2012, 2012.

Knippertz, P., Evans, M. J., Field, P. R., Fink, A. H., Liousse, C. and Marsham, J. H.: The possible role of local air pollution in climate change in West Africa, Nat. Clim. Chang., doi:10.1038/nclimate2727, 2015.

Knippertz, P., Fink, A. H., Deroubaix, A., Morris, E., Tocquer, F., Evans, M. J., Flamant, C., Gaetani, M., Lavaysse, C., Mari, C., Marsham, J. H., Meynadier, R., Affo-Dogo, A., Bahaga, T., Brosse, F., Deetz, K., Guebsi, R., Latifou, I., Maranan, M., Rosenberg, P. D. and Schlueter, A.: A meteorological and chemical overview of the DACCIWA field campaign in West Africa in June-July 2016, Atmos. Chem. Phys., 17(17), 10893–10918, doi:10.5194/acp-17-10893-2017, 2017.

Knote, C., Brunner, D., Vogel, H., Vogel, B. and Lohmann, U.: Online-coupled chemistry and aerosols: COSMO-ART model performance, 2010.

Konare, A., Zakey, A. S., Solmon, F., Giorgi, F., Rauscher, S., Ibrah, S. and Bi, X.: A regional climate modeling study of the effect of desert dust on the West African monsoon, J. Geophys. Res. Atmos., 113(12), 1–15, doi:10.1029/2007JD009322, 2008.

Kreidenweis, S., Zhang, Y. and Taylor, G. R.: The Effects of Clouds on Aerosol and Chemical Species Production and Distribution. Part III: Aerosol Model Description and Sensitivity Analysis, J. Geophys. Res., 102(27), 23,867-23,882, doi:10.1175/1520-0469(1998)055<0921:teocoa>2.0.co;2, 1997.

Lelieveld, J., Fnais, M., Evans, J. S., Giannadaki, D. and Pozzer, A.: The contribution of outdoor air pollution sources to premature mortality on a global scale, Nature, 525(7569), 367–371, doi:10.1038/nature15371, 2015.

https://doi.org/10.5194/acp-2019-617
Preprint. Discussion started: 9 August 2019


Liousse, C., Assamoi, E., Criqui, P., Granier, C. and Rosset, R.: Explosive growth in African combustion emissions from 2005 to 2030, Environ. Res. Lett., doi:10.1088/1748-9326/9/3/035003, 2014.

Marais, E. A. and Wiedinmyer, C.: Air Quality Impact of Diffuse and Inefficient Combustion Emissions in Africa (DICE-Africa), Environ. Sci. Technol., doi:10.1021/acs.est.6b02602, 2016.

Mari, C., Jacob, D. J. and Bechtold, P.: Transport and scavenging of soluble gases in a deep convective cloud, J. Geophys. Res. Atmos., doi:10.1029/2000JD900211, 2000.

Mari, C. H., Cailley, G., Corre, L., Saunois, M., Attié, J. L., Thouret, V. and Stohl, A.: Tracing biomass burning plumes from the Southern Hemisphere during the AMMA 2006 wet season experiment, Atmos. Chem. Phys., 8(14), 3951–3961, doi:10.5194/acp-8-3951-2008, 2008.

Menut, L., Flamant, C., Turquety, S., Deroubaix, A., Chazette, P. and Meynadier, R.: Impact of biomass burning on pollutant surface concentrations in megacities of the Gulf of Guinea, Atmos. Chem. Phys., 18(4), 2687–2707, doi:10.5194/acp-18-2687-2018, 2018.

N'Datchoh, E. T., Konaré, A., Diedhiou, A., Diawara, A., Quansah, E., Assamoi, P. and .: Effects of climate variability on savannah fire regimes in West Africa, Earth Syst. Dyn., 6(1), 161–174, doi:10.5194/esd-6-161-2015, 2015.

N'Datchoh, E. T., Diallo, I., Konaré, A., Silué, S., Ogunjobi, K. O., Diedhiou, A. and Doumbia, M.: Dust induced changes on the West African summer monsoon features, Int. J. Climatol., 38(1), 452–466, doi:10.1002/joc.5187, 2018.

Pan, L., Gille, J. C., Edwards, D. P., Bailey, P. L. and Rodgers, C. D.: Retrieval of tropospheric carbon monoxide for the MOPITT experiment, J. Geophys. Res. Atmos., 103(D24), 32277–32290, doi:10.1029/98JD01828, 1998.

Parker, D. J., Burton, R. R., Diongue-Niang, A., Ellis, R. J., Felton, M., Taylor, C. M., Thorncroft, C. D., Bessemoulin, P. and Tompkins, A. M.: The diurnal cycle of the West African monsoon circulation, Q. J. R. Meteorol. Soc., 131(611), 2839–2860, doi:10.1256/qj.04.52, 2005.

Platnick, S., Meyer, K. G., King, M. D., Wind, G., Amarasinghe, N., Marchant, B., Arnold, G. T., Zhang, Z., Hubanks, P. A., Holz, R. E., Yang, P., Ridgway, W. L. and Riedi, J.: The MODIS Cloud Optical and



Microphysical Products: Collection 6 Updates and Examples from Terra and Aqua, IEEE Trans. Geosci. Remote Sens., 55(1), 502–525, doi:10.1109/TGRS.2016.2610522, 2017.

Raji, K. B., Ogunjobi, K. O. and Akinsanola, A. A.: Radiative effects of dust aerosol on West African climate using simulations from RegCM4, Model. Earth Syst. Environ., 3(1), 34, doi:10.1007/s40808-017-0295-y, 2017.

Sekou, K.: Docteur de l'Université Félix Houphouët-Boigny., 2018.

Solmon, F., Mallet, M., Elguindi, N., Giorgi, F., Zakey, A. and Konaré, A.: Dust aerosol impact on regional precipitation over western Africa, mechanisms and sensitivity to absorption properties, Geophys. Res. Lett., 35(24), doi:10.1029/2008GL035900, 2008.

Stanelle, T., Vogel, B., Vogel, H., Bäumer, D. and Kottmeier, C.: Feedback between dust particles and atmospheric processes over West Africa during dust episodes in March 2006 and June 2007, Atmos. Chem. Phys., 10(22), 10771–10788, doi:10.5194/acp-10-10771-2010, 2010.

Stowe, L. L., Jacobowitz, H., Ohring, G., Knapp, K. R. and Nalli, N. R.: The Advanced Very High Resolution Radiometer (AVHRR) Pathfinder Atmosphere (PATMOS) climate dataset: Initial analyses and evaluations, J. Clim., 15(11), 1243–1260, doi:10.1175/1520-0442(2002)015<1243:TAVHRR>2.0.CO;2, 2002.

Vogel, B., Vogel, H., Bäumer, D., Bangert, M., Lundgren, K., Rinke, R. and Stanelle, T.: The comprehensive model system COSMO-ART – Radiative impact of aerosol on the state of the atmosphere on the regional scale, Atmos. Chem. Phys., 9(22), 8661–8680, doi:10.5194/acp-9-8661-2009, 2009.

Walter, C., Freitas, S. R., Kottmeier, C., Kraut, I., Rieger, D., Vogel, H. and Vogel, B.: The importance of plume rise on the concentrations and atmospheric impacts of biomass burning aerosol, Atmos. Chem. Phys., doi:10.5194/acp-16-9201-2016, 2016.

Van der Werf, G. R., Randerson, J. T., Collatz, G. J. and Giglio, L.: Carbon emissions from fires in tropical and subtropical ecosystems, Glob. Chang. Biol., 9(4), 547–562, doi:10.1046/j.1365-2486.2003.00604.x, 2003.

Wu, M. L. C., Reale, O., Schubert, S. D., Suarez, M. J., Koster, R. D. and Pegion, P. J.: African easterly jet: Structure and maintenance, J. Clim., doi:10.1175/2009JCLI2584.1, 2009.

Yin, Y., Parker, D. J. and Carslaw, K. S.: Simulation of trace gas redistribution by corrective clouds - Liquid

https://doi.org/10.5194/acp-2019-617
Preprint. Discussion started: 9 August 2019


Atmospheric Chemistry and Physics Discussions

phase processes, Atmos. Chem. Phys., 1(1), 19–36, doi:10.5194/acp-1-19-2001, 2001.

Zängl, G., Reinert, D., Rípodas, P. and Baldauf, M.: The ICON (ICOsahedral Non-hydrostatic) modelling framework of DWD and MPI-M: Description of the non-hydrostatic dynamical core, Q. J. R. Meteorol. Soc., 141(687), 563–579, doi:10.1002/qj.2378, 2015.

Zuidema, P., Redemann, J., Haywood, J., Wood, R., Piketh, S., Hipondoka, M. and Formenti, P.: Smoke and clouds above the southeast Atlantic: Upcoming field campaigns probe absorbing aerosol's impact on climate, Bull. Am. Meteorol. Soc., 97(7), 1131–1135, doi:10.1175/BAMS-D-15-00082.1, 2016.